# Correlation dynamics and enhanced signals for the identification of serial biomolecules and DNA bases

**Towfiq Ahmed**[1,7]**, Jason T Haraldsen**[1,2,3]**, John J Rehr**[4]**,**
**Massimiliano Di Ventra**[5]**, Ivan Schuller**[5] **and Alexander V Balatsky**[1,2,6,7]

[1] Theoretical Division, Los Alamos National Laboratory, Los Alamos, NM 87545, USA

[2] Center for Integrated Nanotechnologies, Los Alamos National Laboratory, Los Alamos, NM 87545, USA

[3] Department of Physics and Astronomy, James Madison University, Harrisonburg, VA 22807, USA

[4] Department of Physics, University of Washington, Seattle, WA 98195, USA

[5] Department of Physics, University of California, San Diego, CA 92093, USA

[6] Nordic Institute of Theoretical Physics, KTH Royal Institute of Technology and Stockholm University, Stockholm, Sweden

E-mail: atowfiq@u.washington.edu, haraldjt@jmu.edu, jjr@uw.edu, diventra@physics.ucsd.edu, ichuller@physics.ucsd.edu and balatsky@hotmail.com

## Abstract

Nanopore-based sequencing has demonstrated a significant potential for the development of fast, accurate, and cost-efficient fingerprinting techniques for next generation molecular detection and sequencing. We propose a specific multilayered graphene-based nanopore device architecture for the recognition of single biomolecules. Molecular detection and analysis can be accomplished through the detection of transverse currents as the molecule or DNA base translocates through the nanopore. To increase the overall signal-to-noise ratio and the accuracy, we implement a new 'multi-point cross-correlation' technique for identification of DNA bases or other molecules on the single molecular level. We demonstrate that the cross-correlations between each nanopore will greatly enhance the transverse current signal for each molecule. We implement first-principles transport calculations for DNA bases surveyed across a multilayered graphene nanopore system to illustrate the advantages of the proposed geometry. A time-series analysis of the cross-correlation functions illustrates the potential of this method for enhancing the signal-to-noise ratio. This work constitutes a significant step forward in facilitating fingerprinting of single biomolecules using solid state technology.

Keywords: graphene nanopore, cross-correlation, tunneling conductance, electronic DNA sequencing, DFT NEGF calculation

⑤ Online supplementary data available from stacks.iop.org/Nano/25/125705/mmedia

(Some figures may appear in colour only in the online journal)

## 1. Introduction

With applications ranging from explosives and drug detection to DNA sequencing and biomolecular identification, the ability to detect specific molecules and/or molecular series presents many challenges for scientists. With a specific need for timely and accurate measurements and evaluation, it is essential that researchers both investigate the manner of detection and explore new and improved computational methods for analysis to keep up with the growing pace of the individual fields.

---

[7] Authors to whom any correspondence should be addressed.

The field of single-molecule sequencing is rapidly evolving due to increasing support and technology. As this occurs, sequencing techniques are challenged by the need for a rapid increase of accuracy, speed, and resolution for smaller amounts of material [1, 2]. Nanopore-based sequencing [3–5] and scanning tunneling microscopy based serial methods [6–8] provide promising alternatives to the well-established Sanger method [9], particularly for identifying single DNA bases using transverse conductance [10, 11]. Such an approach relies on the ability to resolve the electronic fingerprints of DNA one relevant unit at a time ('serial') as DNA translocates through a nanochannel. It has been established that experimental methods are capable of achieving single-base resolution, which has prompted investigations into the local electrical properties of single DNA bases [12]. Concurrently, the theoretical underpinnings of this approach have been continuously developing [6, 13, 7, 10, 11].

The single-molecule sensitivity of nanopore sequencing has been recently demonstrated by Kawai *et al* [14] and Lindsay *et al* [15], while the sequence of DNA/RNA oligomers and microRNA by tunneling has also been demonstrated [16]. Despite high-quality experimental methods, the most pressing challenge in serial sequencing lies in overcoming effects of noise that lead to a small signal-to-noise (S/N) ratio in the measured current $I$. The signal fluctuations generally originate from thermal agitation and bond formation between base and nanopore/electrode walls or interactions with a substrate. In an effort to avoid these limitations, we propose the sequential measurement of transverse current cross-correlations, as obtained from multiple pairs of electrodes. The experimental setup for such a nanopore arrangement is schematically shown in figure 1. To be specific, we focus on graphene as the porous material, because it is atomically thick and exhibits extraordinary thermal and electronic properties. Besides these geometric advantages and good conductivity, graphene also possesses high tensile strength and can endure a high transmembrane pressure environment [17]. Consequently, graphene has been proposed as an effective substrate and conducting medium for nanopore and nanogap sequencing by numerous groups [18–20]. We emphasize, however, that the method for nanopore sequencing may be useful in any other method in which serial measurements (e.g., time series) are made to ascertain individual properties (resistivity here) of the bases.

Although this challenge is much more severe for protein based or solid state nanopores, the nature of an atomically thick graphene nanopore wall cannot completely rule out the $\pi$–$\pi$ stacking between carbon and DNA bases. In addition, vibration and other electronic fluctuations present in the graphene membrane can significantly mask the conductance signals, making it difficult to differentiate the individual DNA bases. Previous theoretical [7, 13] studies of the interactions between DNA bases and graphene derivatives have revealed the local electronic structure of single bases. Theoretical [21–23] and experimental [24–26] study of DNA translocation through graphene nanopores has been reported by several groups. Theoretical simulation of DNA sequencing with a graphene-based nanochannel device was performed by Min *et al* [27]. The experimental realization of a single layer
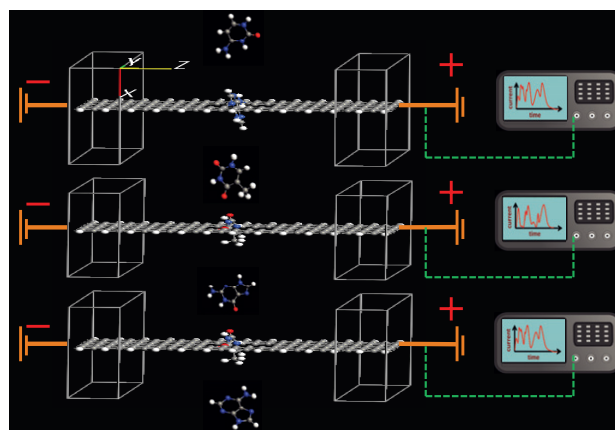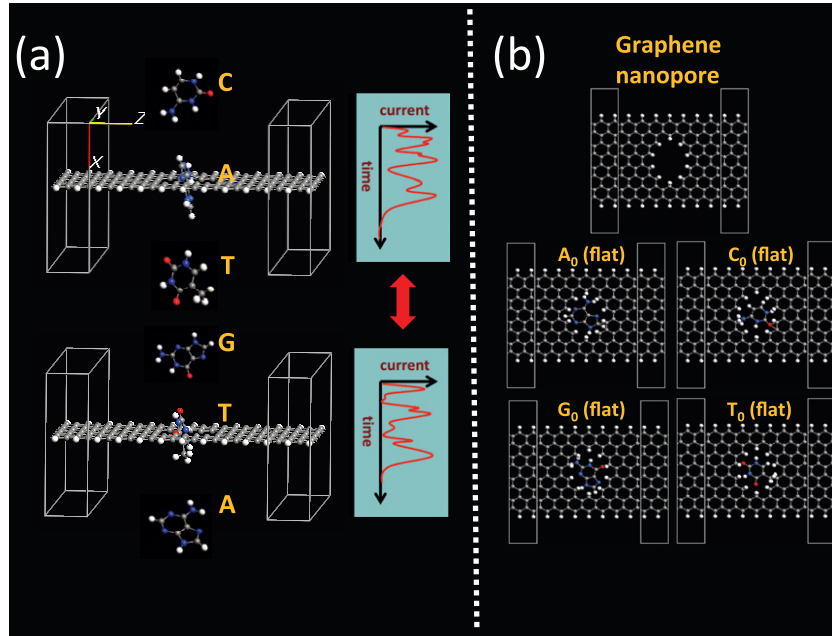


**Figure 1.** Schematic representation of multilayered graphene nanopore device where isolated DNA bases pass through the nanopores. The current versus time spectra are recorded for each layer independently.

graphene-based nanopore device is made possible by combining several state of the art techniques, e.g., exfoliation from graphite on $SiO_2$ substrate [24, 28]. Theoretical simulations of scanning tunneling spectroscopy (STS) [6] support the identification of electronic features with varying spatial extent and intensity near the HOMO-LUMO band.

To make nanopore sequencing and detection a viable method for determining translocating molecules, one must overcome the noise-to-signal problem. Therefore, we propose a multilayered graphene device in which the transverse conductance is measured through each nanopore independently, as a series of DNA bases or other molecules translocates through them (see figure 1). As molecules translocate, they create a time-dependent sequence of translocation currents through each of the layers. One then monitors the translocation currents at different pores and acquires a record of sequential current of the same base as it arrives and moves through the individual pores (shown in figure 2). The time series of the cross-correlation currents can then be used to reduce the uncorrelated independent noise source, and hence enhance the signal-to-noise ratio and improve the differentiation between bases. While our device is being discussed under the idea of DNA sequencing and biomolecules, the general method and device setup can be used for any molecule small enough to fit through a nanopore. This cross-correlation method for data analysis of the transverse currents can be utilized for the analysis of any molecular series given the proper understanding of the molecules' electronic properties.

## 2. Computational method

In this work, we ignore the background contribution from the large phosphate backbone that is typically present in a single-stranded DNA (ssDNA). This simplification is based on the assumption that by identifying and subtracting the background noise coming from the heavy and rigid backbone structure one can isolate the relevant signal from the individual bases. More specifically, we have built on earlier work [6, 13, 10, 20] to model the pore conductance containing

**Figure 2.** (a) Schematic of transmission currents through two graphene layers where isolated DNA bases pass through the nanopores. The current versus time spectra are recorded for each layer independently. A cross-correlation between the current data from multipores reveals useful information by increasing signal-to-noise ratio as described in the text. (b) Hydrogen capped graphene nanoribbons and the DNA bases inside the pore. Here, only the flat orientation of the DNA bases is shown.

a molecule in two steps, as follows. (1) First, we carried out *ab initio* calculations of transmission ($T(E)$) and current ($I$) as a single DNA base translocates through the nanopore of a graphene mono-layer. (2) Then, we simulate the time dependence of the current data by adopting a simple model with multilayered graphene nanopores with added statistical noise and broadening.

Calculations of transmission were performed by taking each DNA base inside the nanopore with three different angular orientations, and using the Landauer–Buttikker [29] formalism implemented in the *ab initio* software atomistic toolkit (ATK) [30]. We emphasize that our approach does not rely upon a geometry optimization of molecules in the pores.The translocation is a dynamical process with significant variations of configurations found for molecules inside a pore. Thus, the same molecule can arrive in different orientations at each pore, a process which contributes to the configuration noise sources that we address here. Therefore, we do not optimize the configurations and instead use the set of various configurations as the set, from which the random sampling is taken.

In these calculations, we have taken a graphene nanoribbon with 208 carbon atoms in the conduction region and constructed a nanopore by removing the center carbon atoms and capping the inner wall with hydrogen atoms, since hydrogenated edges were found [20] to enhance the average experimental conductivity. In this work, the nanopore [19] and nanogap [18] dimension is much smaller than that modeled by other groups. While current nanopore fabrication is limited to larger nanopore sizes, our average nanopore diameter (0.85 nm) is comparable to the nanogap diameter reported by Scheicher *et al* [20] (1.1 nm). We believe the size of

our nanopore is small enough to properly allow only single molecular DNA bases to translocate. In figure 2(b), we only show the flat orientation of the base with the maximum areal projection on the graphene plane. Other angular configurations will require a smaller passage through the pore. We emphasize that such a nanopore size is suitable for single biomolecular detection, which is a single DNA base in this case. While this does not exclusively require nanopore access for a single nucleotide with sugar and phosphate, the multilayered device geometry and cross-correlation are independent of this choice. To determine electrical transmission, the bias voltage between the left and right electrodes is fixed as +0.35 and −0.35 eV.

We demonstrate the recoverability of current ($I(t)$) signals from noise by showing the relation between noise coming from different layers. For simplicity, we consider the dominant noise primarily from two sources. As the bases translocate through the $i$th graphene nanopore layer, the vibration in the DNA backbone may influence an individual base plane to land with random angular orientation with the graphene plane, causing a configuration noise $S_i^C(t)$. The additional noise, such as thermal vibration of the graphene membrane at the $i$th nanopore, is defined as $S_i^A(t)$. Thus, the total noise of the $i$th nanopore can be expressed as

$$S_i(t) = S_i^C(t) + S_i^A(t). \tag{1}$$

The correlation between the two layers is therefore given by

$$\begin{aligned}
\langle S_i(t) \cdot S_j(t') \rangle = {} & \langle S_i^C(t) \cdot S_j^C(t') \rangle \\
& + \langle S_i^C(t) \cdot S_j^A(t') \rangle + \langle S_i^A(t) \cdot S_j^C(t') \rangle \\
& + \langle S_i^A(t) \cdot S_j^A(t') \rangle. \tag{2}
\end{aligned}$$
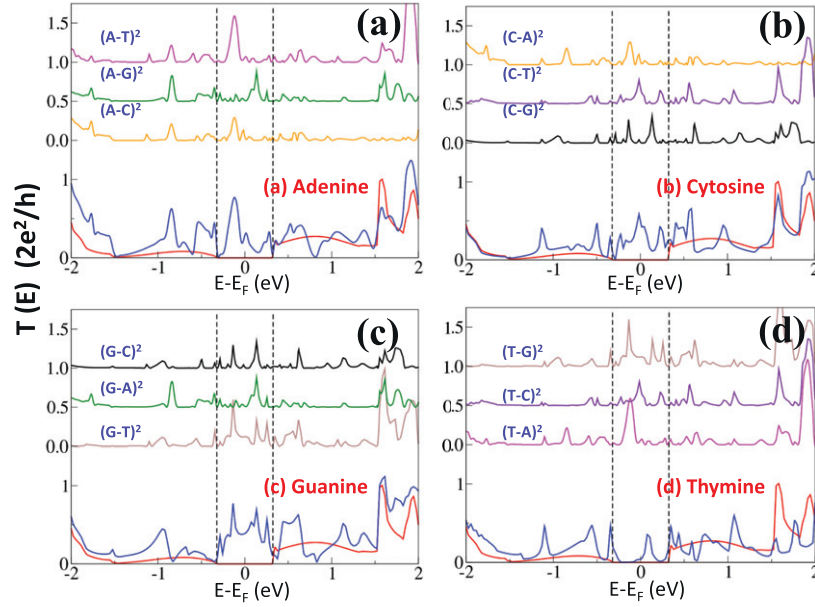
**Figure 3.** Configuration averaged transmission coefficients (solid blue lines) for (a) adenine, (b) cytosine, (c) guanine, and (d) thymine. The solid red line is $T(E)$ for pure graphene with nanopore for comparison. The vertical dashed lines are at $-0.35$ eV and $+0.35$ eV which are the $E_F$ of the left and right electrode respectively. The top three curves in each panel are the difference-square curves between the average $T(E)$ for each base. The Fermi energy of the central region is at 0 eV and the difference curve shows distinguishing features for each of the DNA bases.

Here $t' = t + \Delta t$. For $i \neq j$, the contributions from the last three terms on the right side of equation (2) are negligible due the weakly or uncorrelated signals in separate nanopores. Since the DNA bases are strongly attached to the ssDNA backbone, the configuration noise between two membranes mainly contributes to the first term in equation (2). Therefore, the noise can be approximated as

$$\langle S_i \cdot S_j \rangle \approx \langle S_i^C \cdot S_j^C \rangle, \tag{3}$$

where, for $i = j$, all the terms on the right side of equation (2) survive and contribute significantly to the total noise. Since the noise between $i$ and $j$ is uncorrelated, a comparison of their signals will enhance the individual base signals by reducing the noise-to-signal ratio.

There are two extreme limits in which we can take advantage of the above observation. These limits relate to the rate of base translocation compared to the typical vibrational frequency of the bases facing the electrodes. When this occurs, the above cross-correlations allow us to reduce the *intrinsic* noise due to random orientations. On the other hand, when the translocation rate is slower than the vibrational frequency, the uncorrelated noise is eliminated and the only one that survives is the correlated one. We focus here on the second case, since experimentally, the latter situation is more likely [4, 5].

As an example, we show the low current amplitude for thymine in figure 4(a), and in figure 4(c) the enhancement of the signal-to-noise ratio. We have taken a test sequence $A_0C_0A_2G_2T_1C_2G_1T_2$, where the subscripts imply different angular orientations of the bases inside the pore. The time dependence of this sequence is modeled by taking the time interval between two consecutive bases $\tau = 1.0$ $\mu$s, including

a random Gaussian uncertainly between the interval with $\sigma_\tau = \pm 0.2$ $\mu$s. Each current signal is also broadened using a random Gaussian broadening with $\sigma_{\text{broad}} = 0.2$ $\mu$A. To simulate a realistic experiment with background noise, we have also included additive white Gaussian noise. We assume that with the applied field in the vertical direction, the average elapsed time between two translocating bases is $\tau \approx 1.0$ $\mu$s. The time-distance between two consecutive graphene layers is set to $\Delta t \approx 0.2$ $\mu$s.

## 3. Results and discussion

We first discuss our first-principles calculations of transmittance for individual DNA bases inside the graphene nanopore, as presented in figure 3. Then in figure 4, we show the partial signal recovery using our time-simulation model with three layer graphene nanopores and the cross-correlation between the corresponding signals.

In our first-principles approach, for each DNA base, we have taken three random angular orientations with the graphene membrane, while calculating the transmittance between the two electrodes with 0.7 V bias voltage. The configuration averaged transmittance for A, C, G, and T are shown in the solid blue curve in figures 3(a)–(d). The conductance of a pure graphene nanoribbon with hydrogenated nanopore is shown in the solid red curve in figure 3 for comparison. The transmittance curve is analogous to the non-equilibrium density of states in the presence of the bias voltage where the zero of energy is the Fermi energy of the central graphene region. The vertical dashed lines are at $-0.35$ eV and $+0.35$ eV, which are the chemical potentials of the left and right electrodes
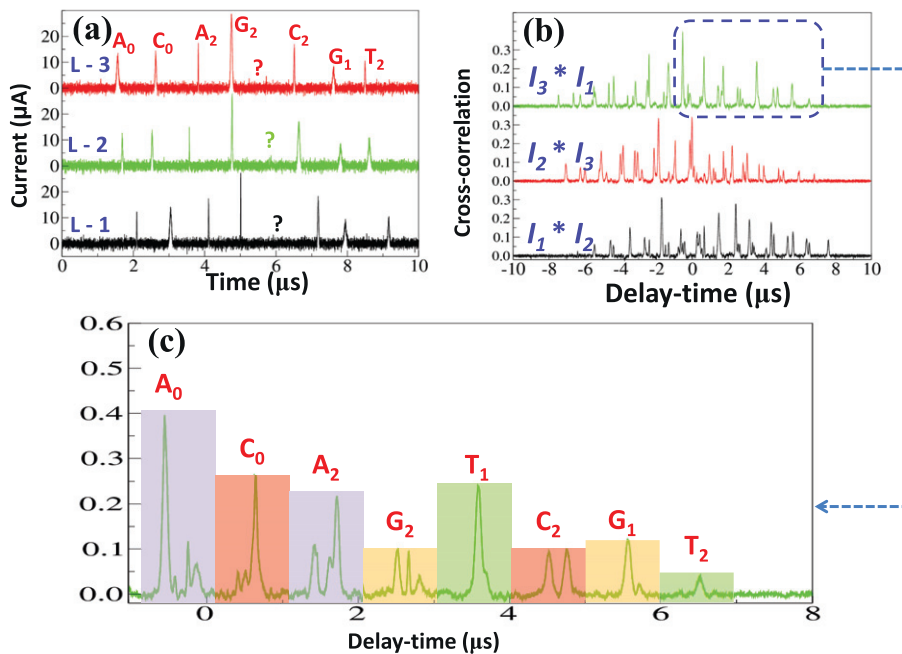
**Figure 4.** (a) Current versus time ($\mu$s) plot for a translocating DNA sequence 'ACAGTCGT' for three graphene layers labeled as L-1, L2, and L-3. An additive white noise is included in the current spectrum. Due to high noise-to-signal ratio some of the spectral features became harder to recognize (indicated by a question mark in the figure). (b) Cross-correlation between current signals $I_1(t)$, $I_2(t)$, and $I_3(t)$ as functions of delay time $\Delta t$, where the currents are from graphene layers L-1, L-2, and L-3 respectively. (c) Enlarged segment of the cross-correlation function from (b). These correlation-signal peaks correspond to the peaks from current signal for the DNA sequence ACAGTCGT.

respectively. For each base (figures 3(a)–(d)), the transmittance curve (solid blue line) in between the left and right electrode chemical potentials is significantly enhanced compared to the pure graphene membrane with a nanopore (solid red line). The features in this region are characteristic of the four bases. For example, a comparison of the guanine transmittance (figure 3(c)) with that of thymine (figure 3(d)), shows the presence of a characteristic broad peak.

It should be noted that the transmittance is not zero for the nanoribbon. The transmittance is simply reduced due to the presence of the nanopore on this modeling scale. Since graphene is conductive and will be able to transmit a current through the ribbon, we are focusing the molecular conductance from the translocating molecules through the nanopore. Therefore, we are simulating a large nanopore on a relatively small ribbon to emphasize the transmittance of the individual bases.

For a systematic study of the differences between the transmittances among the four bases, we also plotted the difference curves (the top three) in figures 3(a)–(d). If the signatures of one or more of the DNA bases are known prior to the detection, the difference curve may provide the signature of an unknown base. For example, if one knows the transmittance of thymine, a comparison of the characteristic features of difference-squared transmittance $(A–T)^2$, $(G–T)^2$, $(C–T)^2$, helps identify the unknown base. In figures 3(a), (c), and (d), they show the difference curves contain several (up to three) dominant peaks in between the vertical dashed

lines. In principle, it is possible to calculate a large number of configurations and maintain a complete data-base of such characteristic difference curves for sequencing purposes.

Such methods are challenged by two major limitations. The first one is prior knowledge of the exact location of one or more kinds of DNA base, either from the transmittance curve or from other techniques. The second one is the presence of significant noise in the data, which makes it difficult for the detection of any single base. Some bases exhibit characteristic features in the transmittance curve, which make them easily detectable. For example, thymine (figure 3(d) solid blue line) has a very low conductance compared to the others which (in agreement with previous calculations [10, 11]) is shown by the low peak amplitude near 0 eV. However, even the detection of thymine can be difficult in the presence of noisy data. To illustrate the specifics of the approach, we present the simulation of a time series for three graphene nanopore layers with the test sequence $A_0C_0A_2G_2T_1C_2G_1T_2$ in figure 4, where, for example, the notations $A_0$, $A_1$ and $A_2$ indicate three different angular orientations of the base adenine with respect to the graphene membrane.

In nanopore-based DNA sequencing, the current ($I(t)$) is the measured quantity rather than the transmittance ($T(E)$). Thus, we calculated the current from the transmittance. Using the parameters described previously we simulated time-dependent current spectra $I_{L-1}$, $I_{L-2}$, and $I_{L-3}$ for our test sequence, as shown in figure 4(a). Here, L-1, L-2 and L-3 indicate graphene layers 1, 2, and 3 respectively. The low
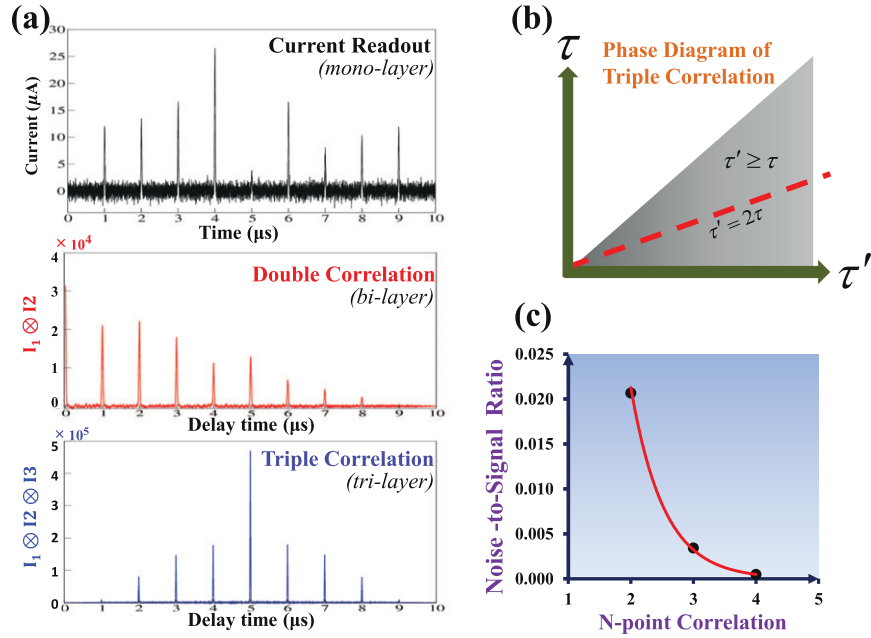
**Figure 5.** The three panels in (a) show the improvements in signal-to-noise ratio, with higher order cross-correlation. The time dependent current spectrum for the sequence $A_0 C_0 A_2 G_2 T_1 C_2 G_1 T_2 C_1$ from single layer graphene is shown in the top panel (black); the double and triple cross-correlated spectra are shown in the middle (red) and bottom (blue) panels. (b) Phase diagram of a triple correlation function in a 2D delay-time parametric space for $\tau$ and $\tau'$. The dashed red line is our constraint for calculating the triple correlation function. (c) Nearly exponential decay of noise-to-signal ratio with higher order correlation.

current amplitude for thymine in the case of $T_1$ and $T_2$ is expected from the transmittance curve in figure 3(d), but the natural noise present in the data makes it difficult to confirm the presence of $T_1$ at the expected location. In figure 4(b), we present the cross-correlation between the current spectra from different pairs of graphene layers. For each pair, the cross-correlation is plotted as a function of time-delay within the $-10$ to $+10$ $\mu$s range. The cross-correlation spectrum is approximately symmetric around the mid point of the total range due to the overlaps between similar pairs of peaks from opposite ends of the original data. Therefore, we only focus on the positive time-delay. The correlation spectrum inside the highlighted dashed box in figure 4(b) is enhanced in figure 4(c). By comparing peaks between figures 4(a) and (c), we confirm the presence of thymine with $T_1$ configuration. Although the amplitudes of the current spectrum do not translate directly into the amplitudes of the cross-correlation spectrum, they confirm the existence of $T_1$. Thus, a time-series analysis using current cross-correlations $\langle I_i(t) \otimes I_j(t) \rangle$ recovers all eight peaks in our test sequence (figure 4(b)). The suppression of white noise is substantial and the peaks at time-delay $= 0$ in the correlation function (figure 4(b)) are enhanced.

We can easily extend this approach to three-point or higher $N$-point correlations, which we demonstrate here, to exponentially reduce the noise-to-signal ratio. The two-point cross-correlation is generally expressed with a single parameter as in

$$R^{(2)}(\tau) = \int_0^T I_1(t) I_2(t-\tau)\, \mathrm{d}t, \tag{4}$$

where the time interval is between $0$ and $T$. The three-point correlation is a function of two independent variables,

$$R^{(3)}(\tau, \tau') = \int_0^T I_1(t) I_2(t-\tau) I_3(t-\tau')\, \mathrm{d}t. \tag{5}$$

We can simplify the description of the triple correlation function in the complete two dimensional parametric space by constraining it to the line $\tau' = 2\tau$ as in figure 5(b). Thus the constrained triple correlation function becomes,

$$R^{(3)}(\tau) = \int_0^T I_1(t) I_2(t-\tau) I_3(t-2\tau)\, \mathrm{d}t. \tag{6}$$

Following this procedure we can measure currents from $N$ independent graphene layers and calculate the constrained $N$-point correlation as

$$R^{(N)}(\tau) = \int_0^T I_1(t) I_2(t-\tau) I_3(t-2\tau)$$
$$\dots I_N(t-(N-1)\tau)\, \mathrm{d}t. \tag{7}$$

The three panels in figure 5(a) show our calculated current signal from a single layer as well as the two and three point cross-correlation functions from the corresponding two and three independent graphene nanopores. The test sequence used here is $A_0 C_0 A_2 G_2 T_1 C_2 G_1 T_2 C_1$. Using two, three, and four point cross-correlation functions, we estimated the ratios between the average signal and average noise in each case, as shown in table 1 in the supplementary section (available at

stacks.iop.org/Nano/25/125705/mmedia). We confirm the exponential drop in the noise to signal ratio as shown in figure 5(c). The computational details and the table containing the results are also given in the supplementary section (available at stacks.iop.org/Nano/25/125705/mmedia).

## 4. Conclusions

We implement first-principles calculation of transmittance for a systematic study of the identification of single DNA bases or other biomolecules translocating through graphene nanopores. While our device is being discussed under the idea of DNA sequencing, the general method and device setup can be used for any molecule small enough to fit through a nanopore. We are focusing on the area of DNA sequencing and biomolecules, but this cross-correlation method for data analysis of the transverse currents can be utilized for the analysis of any molecular series given the proper understanding of the molecules' electronic properties. To eliminate the high background noise, we propose a multilayered graphene-based nanopore device combined with a multi-point cross-correlation method to substantially improve the signal-to-noise ratio of the electronic readout of biomolecules. We adopted a statistical method for simulating the time-dependent current spectrum to illustrate this approach. The enhanced resolution is produced by the multiple translocation readouts of the same bases of the same molecule through the pores. The cross-correlated signals from each pair of electrodes will suppress the uncorrelated noise produced by each single translocation event.

In this way thymine can serve as a 'reference molecule' for identifying other molecules from the change in the transmittance curves. We also demonstrate the recovery of signals associated with different configurations by taking cross-correlations between different pairs of graphene layers. This study provides a promising method for an enhanced signal-to-noise ratio in multipore graphene-based devices (or any other serial sequencing device), and their potential applicability as a next generation biomolecular detection technique. While we focus on the correlations in DNA bases, this cross-correlation method can be used for any molecule or molecular series for detection or identification purposes.

## Acknowledgments

## References

[1] Carlke J, Wu H C, Jayasinghe L, Patel A, Reid S and Bayley H 2009 *Nature Nanotechnol.* **4** 265–70

[2] Kasianowicz J J, Brandin E, Branton D and Deamer D W 1996 *Proc. Natl Acad. Sci. USA* **93** 13770–3

[3] Venkatesan B M and Bashir R 2011 *Nature Nanotechnol.* **6** 615–24

[4] Zwolak M and Di Ventra M 2008 *Rev. Mod. Phys.* **80** 141–65

[5] Branton D *et al* 2008 *Nature Biotechnol.* **26** 1146–53

[6] Ahmed T, Kilina S, Das T, Haraldsen J T, Rehr J J and Balatsky A V 2012 *Nano Lett.* **12** 927–31

[7] Kilina S, Tretiak S, Yarotski D A, Zhu J X, Modine N, Taylor A and Balatsky A V 2007 *J. Phys. Chem.* C **111** 14541–51

[8] Tanaka H and Kawai T 2009 *Nature Nanotechnol.* **4** 518–22

[9] Sanger F, Nicklen S and Coulson A R 1977 *Proc. Natl Acad. Sci. USA* **74** 5463–7

[10] Zwolak M and Di Ventra M 2005 *Nano Lett.* **5** 421–4

[11] Lagerqvist J, Zwolak M and Di Ventra M 2006 *Nano Lett.* **6** 779–82

[12] Yarotski D A, Kilina S V, Talin A A, Tretiak S, Prezhdo O V, Balatsky A V and Taylor A J 2009 *Nano Lett.* **9** 12–7

[13] Kilina S, Yarotski D A, Talin A A, Tretiak S, Taylor A J and Balatsky A V 2011 *J. Drug Deliv.* **2011** 415621

[14] Tsutsui M, Taniguchi M, Yokota K and Kawai T 2010 *Nature Nanotechnol.* **5** 286–90

[15] Chang S, Huang S, He J, Liang F, Zhang P, Li S, Chen X, Sankey O and Lindsay S 2010 *Nano Lett.* **10** 1070–5

[16] Ohshiro T, Matsubara K, Tsutsui M, Furuhashi M, Taniguchi M and Kawai T 2012 *Sci. Rep.* **2** 1070–5

[17] Lee C, Wei X, Kysar J W and Hone J 2008 *Science* **321** 385–8

[18] Postma H W C 2010 *Nano Lett.* **10** 420–5

[19] Nelson T, Zhang B and Prezhdo O V 2010 *Nano Lett.* **10** 3237–42

[20] He Y, Scheicher R H, Grigoriev A, Ahuja R, Long S, Huo Z and Liu M 2011 *Adv. Funct. Mater.* **21** 2674–9

[21] Prasongkit J, Grigoriev A, Pathak B, Ahuja R and Scheicher R H 2011 *Nano Lett.* **11** 1941–5

[22] Saha K K, Drndić M and Nikolić B K 2012 *Nano Lett.* **12** 50–5

[23] Avdoshenko S M, Nozaki D, Gomes da Rocha C, González J W, Lee M H, Gutierrez R and Cuniberti G 2013 *Nano Lett.* **13** 1969–76

[24] Garaj S, Hubbard W, Reina A, Kong J, Branton D and Golovchenko J A 2010 *Nature* **467** 190–3

[25] Schneider G F, Kowalczyk S W, Calado V E, Pandraud G, Zandbergen H W, Vandersypen L M K and Dekker C 2010 *Nano Lett.* **10** 3163–7

[26] Merchant C A *et al* 2010 *Nano Lett.* **10** 2915–21

[27] Min S K, Kim W Y, Cho Y and Kim K S 2011 *Nature Nanotechnol.* **6** 162–5

[28] Allen M J, Tung V C and Kaner R B 2009 *Chem. Rev.* **110** 132–45

[29] Du X, Skachko I, Barker A and Andrei E Y 2008 *Nature Nanotechnol.* **3** 491–5

[30] Brandbyge M, Sørensen M R and Jacobsen K W 1997 *Phys. Rev.* B **56** 14956–9